

# Mechanical and Tribological Characterization of CaCO<sub>3</sub> and CaSO<sub>4</sub> Filled CSM-E-Glass Fiber Reinforced Vinyl Ester Composites

Sandeep Kumar<sup>1\*</sup>, Sant Ram Chauhan<sup>2</sup>

<sup>1</sup>Department of Mechanical Engineering, Lovely Professional University, Phagwara, Punjab, India

<sup>2</sup>Department of Mechanical Engineering, National Institute of Technology, Hamirpur, Himachal Pradesh, India

## Abstract

*In this paper, mechanical and tribological behavior of the composites under dry sliding wear of vinyl ester matrix reinforced with chopped strand mat (CSM)-E-glass fiber and fillers CaSO<sub>4</sub> and CaCO<sub>3</sub> sliding against smooth stainless steel counterface ( $R_a = 0.07 \mu\text{m}$ ) using Taguchi experimental design has been presented. The effects of sliding velocity (1.57, 2.62 and 3.67 m/s), normal load (20, 40 and 60 N), filler content (0, 10 and 20 wt.%) and sliding distance (1000, 3000 and 5000 m) on friction and wear behavior of vinyl ester matrix reinforced with CSM-E-glass fiber composite are measured. An orthogonal array (OA) and analysis of variance (ANOVA) are applied to calculate the influence of process parameters on the coefficient of friction and sliding wear of the composites. The worn surfaces of the polymer composite specimens for each specific test condition are examined using scanning electron microscopy (SEM). The results show that the coefficient of friction and wear rate increases with the increase in the normal load for vinyl ester composite. But, with increasing the filler content the coefficient of friction and wear rate decreases with the increase of normal load.*

**Keywords:** glass fiber, vinyl ester, fillers, scanning electron microscopy, Taguchi technique

\*Author for Correspondence Email: sandeep6437@gmail.com

## INTRODUCTION

The study of sliding wear and coefficient of friction of polymers in general and polymer-based systems in particular is finding increasing interest towards polymer composites. This is due to their light weight, good strength, good corrosion resistance, wider choice of the materials, dimensional stability, high impact strength and ease of manufacturing. An area where their use has been found to be very effective is the situation involving sliding contact wear. Also, the polymer-based materials are preferred in recent years over metal-based composites due to their low coefficient of friction and ability to sustain loads [1, 2]. Tribological performances of the polymer-based composite materials are generally sensitive to the operating and test conditions [3]. Therefore,

experimental tests for predicting the coefficient of friction and wear rate are difficult owing to many test parameters that can affect the tribological properties [4]. This should be expected due to the changes of different factors and their levels that dictate polymer friction and their wear properties including polymer molecular structure, properties, surface texture, mating surface properties, environmental and operating conditions [5–11]. Polymer composites are also increasingly used for a number of mechanical components such as brakes, clutches, bearings, gears, cams, wheels and bushes, most of which are subjected to tribological loading conditions [12]. Polymer composites containing different fillers and reinforcements are frequently used for applications like automotive parts, gear

assemblies, tub/shower industries, etc., in which friction and wear are critical issues. Calcium carbonate ( $\text{CaCO}_3$ ) and calcium sulfate ( $\text{CaSO}_4$ ) are the fillers, which are used in the automobile parts and tub/shower industries respectively.

The importance of tribological properties has convinced many researchers to study the friction and wear behavior and to improve the wear resistance of polymer-based composites. In polymer-based composite materials reinforced with fibers, the process of material removal in dry sliding condition is dominated by four wear mechanisms such as matrix wear, fiber sliding wear, fiber fracture and interfacial debonding [13]. The tribological properties were found to depend on the type of resins, size, shape and orientation of fibers used for reinforcement. One of the preliminary investigations on the effect of fiber-reinforced composites was reported by sung *et al.* [14]. However, in most of the research work, bi-directional fiber with polyester and epoxy

matrix resins is used by the researchers for the study of friction and wear behavior. Only very few researchers have used vinyl ester matrix and CSM-E-glass fiber for the tribological behavior of polymer composites. Chauhan *et al.* [12, 15] used vinyl ester matrix and E-glass fiber to study the sliding friction and wear behavior of vinyl ester and its composites under dry and water-lubricated sliding conditions. They also studied the effect of fly ash content on friction and dry sliding wear behavior of glass fiber-reinforced polymer composites using Taguchi approach. Tayeb *et al.* [4, 16] used CSM 450-R-glass fiber and studied the tribological studies of polyester matrix against smooth stainless steel counterface. From the above mentioned literature, it is understood that there is tremendous potentials of these fillers used for research on glass vinyl ester composites and studied under dry sliding conditions. The chemical structure of vinyl ester resin is shown in Figure 1.

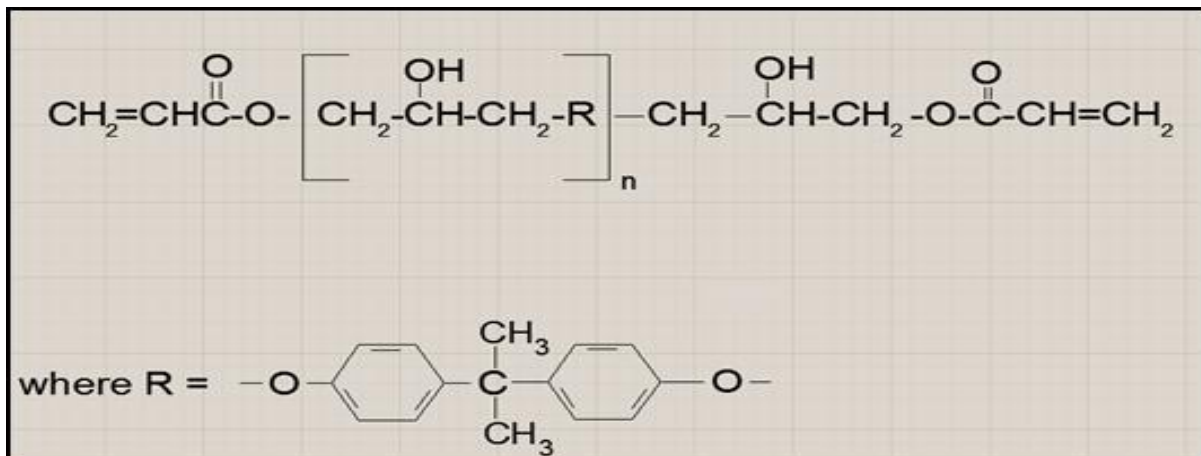


Fig. 1: Chemical Structure of Vinyl Ester Resin.

## EXPERIMENTAL DETAILS

### Materials

Chopped strand mat (CSM)-E-glass fiber was selected as a reinforcement material and vinyl ester as a thermosetting resin material. Glass fiber is a mixture of oxides. The principal oxide is silica with varying smaller amounts of calcium, aluminum, sodium, boron, iron, etc. There are several commercial grades of glass fiber of which the following are the most common such as E, C, S, R, A, D, L. E-glass fiber stands for good electrical insulator and high strength. The CSM is a sheet of reinforcement material comprising of

randomly dispersed chopped fibers held together with a resinous binder. CSM is produced in a variety of lengths, widths and weights. The current chopped strand mat has 40–50 mm fiber lengths and  $300\text{g}/\text{m}^2$  mass of fiber. Vinyl esters are similar to polyesters in that they cure by radical initiated polymerization. They are derived from the reaction of an epoxy resin with acrylic or methacrylic acid and properties can be varied by using different epoxy resins. They are generally tougher, have improved chemical resistance and are capable of higher operating temperatures than polyesters. They fall

between polyesters and epoxies in terms of performance and cost [17].

### Specimen Preparation

The matrix used in this work is vinyl ester resin (density 1.28 g/cc) and CSM-E-glass fiber as a reinforcement material (modulus 72.4 GPa, density 2.54 g/cm<sup>3</sup>) were supplied by Northern Polymer Pvt. Ltd. New Delhi. Methyl ethyl ketone peroxide (MEKP-1.5%) and Cobalt Naphthenate (1.5%) were used as catalyst and accelerator respectively. Three different types of composites are prepared for the study. The Calcium Sulfate (CaSO<sub>4</sub>) and Calcium Carbonate (CaCO<sub>3</sub>) having particle size 1.813 μm and 1.620 μm respectively were used as a filler material collected from the Pioneer Chemical Corporation, Delhi.

Conventional hand lay-up technique has been used for making the polymer composites. The accelerator Cobalt Naphthenate 1.5% is mixed thoroughly in vinyl ester resin and then catalyst 1.5% Methyl ethyl ketone peroxide (MEKP) was mixed in the resins prior to reinforcement. The fiber loading (weight fraction of glass fiber in the composite) is kept 50 wt.% for all the samples. Each ply of fiber

is of dimension 300 × 300 mm<sup>2</sup>. A Silicon rubber sheet was used as model for making the composites. Before lay-up, the mold is sprayed with a release agent (silicon spray) to ensure that the part will not adhere to the mold after the curing of the composites. The alternative layers of the matrix and reinforcement material were laid in the mold. A metal roller was used to impregnate the fibers with the resin so that uniform thickness and compactness could be obtained. Utmost care had been taken to maintain uniformity and homogeneity of the composites fabricated. This procedure was repeated in all cases until thickness of 3 mm was obtained. The cast of each composite is cured under a load of about 40 kg for 48 h at room temperature before it is removed from the mold. During the fabrication of the composites, we found that the curing of the composite also depends on the weathering conditions at room temperature because if we made any composite in winter season then curing time of that composite will take twice the time than that of summer season. Specimens of suitable dimensions are cut using a diamond cutter for sliding wear testing and also for the testing of mechanical properties as per ASTM standard.

**Table 1:** Composition and Designation of the Composites.

Designation	Detail of composition
CGV <sub>1</sub>	Vinyl ester + 50 wt.% CSM-E-glass fiber
CGV <sub>2</sub>	Vinyl ester + 50 wt.% CSM-E-glass fiber + 10 wt.% CaSO <sub>4</sub>
CGV <sub>3</sub>	Vinyl ester + 50 wt.% CSM-E-glass fiber + 20 wt.% CaSO <sub>4</sub>
CGV <sub>4</sub>	Vinyl ester + 50 wt.% CSM-E-glass fiber + 10 wt.% CaCO <sub>3</sub>
CGV <sub>5</sub>	Vinyl ester + 50 wt.% CSM-E-glass fiber + 20 wt.% CaCO <sub>3</sub>

The other composite samples with fillers CaSO<sub>4</sub> and CaCO<sub>3</sub> of fixed weights (10 and 20 wt.%) percentage were fabricated by the same technique. The CaSO<sub>4</sub> and CaCO<sub>3</sub> were mixed thoroughly in the vinyl ester resin mechanically before the CSM-E-glass fiber was reinforced in the matrix body. The composites prepared for this study are designated as CGV<sub>1</sub>, CGV<sub>2</sub>, CGV<sub>3</sub>, CGV<sub>4</sub>, CGV<sub>5</sub> respectively and percentage of fiber content in all the composites is 50 wt.%. The composition and designation of the composites prepared for this study are listed in Table 1.

### Test Apparatus

To evaluate the friction and sliding wear of CSM-E-glass fiber vinyl ester composites, the wear tests are carried out in a pin-on-disc type friction and wear monitoring test rig (DUCOM) as per ASTM G 99. The counter surface is a disc made of hardened ground steel (EN-32, hardness 72 HRC, surface roughness R<sub>a</sub> = 0.07 μm). The specimen was held stationary and the disc was rotated while a normal force was applied through a lever mechanism. The schematic diagram of the pin-on-disc apparatus is shown in Figure 2.

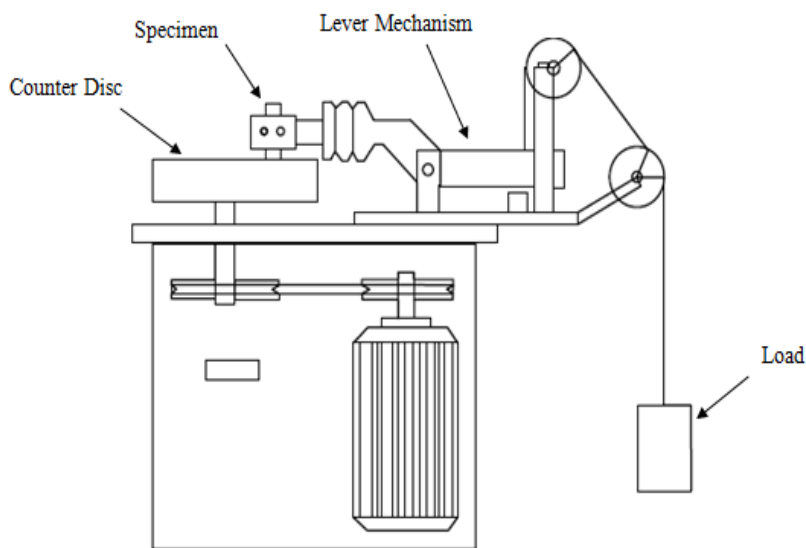


Fig. 2: Schematic Diagram of Pin-on-Disc Apparatus.

During the test, frictional force was measured by the transducer mounted on the loading arm. The frictional force readings were taken as the average of 100 readings of every 40 s for the required time period. For this purpose, a microprocessor-controlled data acquisition system was used. The average mass loss was used to calculate the specific wear rate ( $K_s$ ). The tests were conducted with sliding velocity (1.57, 2.62, 3.67 m/sec.), normal load (20, 40, 60 N), filler content (0, 10, 20%) for the sliding distance of 1000, 3000 and 5000 m. Sliding wear data reported here is the average of two runs. The initial weight before run and final weight after run is measured using a

precision electronic balance with an accuracy of  $\pm 0.01$  mg. The specific wear rate ( $\text{mm}^3/\text{Nm}$ ) is then expressed on “volume loss” basis.

$$K_s = \frac{\Delta m}{L \rho F_n}$$

where,  $K_s$  is the specific wear rate ( $\text{mm}^3/\text{Nm}$ ),  $\Delta m$  is the mass loss in the test duration in grams,  $\rho$  is the density of the composite ( $\text{g}/\text{cm}^3$ ),  $F_n$  is the applied normal load (N),  $L$  is the sliding distance (m). The parameters setting and levels for various control factors for wear tests are shown in Table 2.

Table 2: Parameters Setting and Levels for Various Control Factors for Wear Test.

Control factors	Symbols	Units	Levels		
			I	II	III
Velocity	A	m/s	1.57	2.62	3.67
Normal load	B	N	20	40	60
Filler content	C	%	0	10	20
Sliding distance	D	m	1000	3000	5000

**Experimental Design**

Taguchi design of experiment is a powerful analysis tool which is adopted for optimizing design parameters. Taguchi method provides the designer with a systematic and efficient approach for experimentation to determine near-optimum settings of design parameters

for performance, quality and cost [18–21]. In the conventional full factorial experimental design, it would require  $3^4 = 81$  runs to study four factors each at three levels whereas Taguchi’s factorial experiment approach reduces it to only 27 runs offering a great advantage in terms of experimental time and

cost. The experimental observations are transformed into a signal-to-noise (S/N) ratio. There are three S/N ratios available depending upon the type of characteristics (smaller-the-better, larger-the-better, nominal-the-better). The S/N ratio for minimum (friction and wear rate) coming under smaller-the-better characteristic can be calculated as a logarithmic transformation of the loss function as shown below [22]:

$$\frac{S}{N} = -10 \log \left[ \frac{1}{n} (y_1^2 + y_2^2 + \dots + y_n^2) \right] \quad (1)$$

where “n” is the repeated number trial conditions and  $y_1, y_2, \dots, y_n$  are the response of the friction and sliding wear characteristics. “Lower-the-better” (LB) characteristic, with the above S/N ratio transformation is suitable for minimizations of coefficient of friction and specific wear rate. The standard linear graph is used to assign the factors and interactions to various columns of the orthogonal array (OA).

The plan of experiments is as follows: the first column is assigned to the velocity (A), the second column to normal load (B), the fifth column to filler content (C) and the ninth column to sliding distance (D), the third and fourth columns are assigned to  $(A \times B)_1$  and  $(A \times B)_2$  respectively to estimate interaction between the velocity (A) and the normal load (B), the sixth and seventh columns are to  $(B \times C)_1$  and  $(B \times C)_2$  respectively to estimate the interaction between the normal load (B) and the filler content (C), the eighth and eleventh columns are assigned to  $(A \times C)_1$  and  $(A \times C)_2$  respectively to estimate the interaction between velocity (A) and the filler content (C) and the remaining columns are used to estimate the experimental error. The linear graph for  $L_{27}$  array is shown in Figure 3.

### Scanning Electron Microscopy (SEM)

An FEI quanta FEG450 was used to analyze the worn surfaces of the polymer composites. The composite samples are mounted on stubs with gold plating. To enhance the conductivity of the samples, thin films of platinum are vacuum evaporated onto them before the photomicrographs are taken.

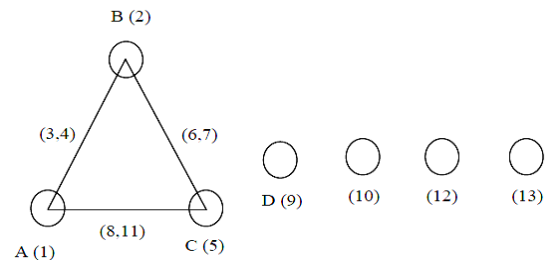


Fig. 3: Linear Graphs for  $L_{27}$  Array.

## RESULTS AND DISCUSSION

The characterization of the composites reveals that inclusion of any particulate filler has very strong influence not only on the mechanical properties of composites but also on their sliding wear behavior. A comparative study of modified behavior of the composites against the unfilled composite and between two different types of fillers is presented.

### Density

The composite under this investigation consists of three components such as matrix, fiber and particulate filler. Hence, the density of the composite can be calculated using rule-of-mixture as shown in the following expression [23]:

$$\rho_{\text{composite}} = \frac{1}{\left(\frac{W_m}{\rho_m}\right) + \left(\frac{W_f}{\rho_f}\right) + \left(\frac{W_p}{\rho_p}\right)} \quad (2)$$

where,  $W$  and  $\rho$  represent the weight fraction and density respectively. The suffix m, f, and p stand for the matrix, fiber and particulate filler respectively. The actual or experimental density ( $\rho_{\text{exp}}$ ) of the composite, however, can be determined by the simple water immersion technique (Archimedes principle). The volume fraction of voids ( $V_v$ ) in the composites is calculated using the following equation:

$$V_v = \frac{\rho_{\text{ct}} - \rho_{\text{exp}}}{\rho_{\text{exp}}} \quad (3)$$

### Mechanical Properties

The tensile test is performed on the universal testing machine (UTM) Hounsfield H25KS as per ASTM standard D 3039-76 [24]. It is seen that in all the samples, irrespective of the filler material, the tensile strength of the composite decreases with increase in filler content.

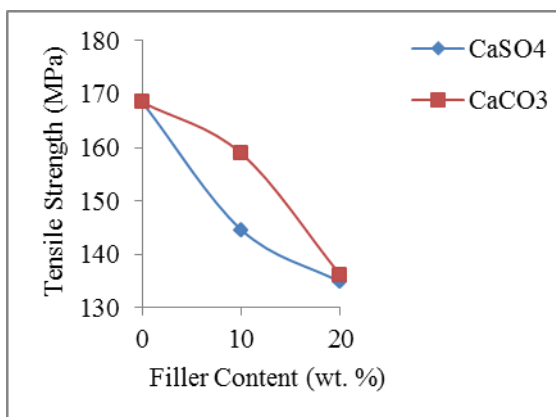


**Fig. 4:** Variation of Tensile Strength of Composites with Filler Type and Content.

The unfilled CSM-E-glass vinyl ester composite (50wt.% fibers loading) has a strength of 168.5 MPa in tension and this value drops to 144.6 and 134.8 MPa with addition of 10 and 20 wt.% of CaSO<sub>4</sub> filler respectively. The same phenomenon has been seen in CaCO<sub>3</sub> filler, the values drop to 158.9 and 136.1 MPa with the addition of the 10 wt.% and 20 wt.% of CaCO<sub>3</sub> filler as shown in Figure 4. Among the two fillers taken in this study, the inclusion of CaSO<sub>4</sub> filler causes maximum reduction in the composite strength.

There can be three reasons for this decrease in the strength properties of these particulate-filled composites compared to the unfilled one. The first possibility is that the interface bonding between the filler particles and the matrix may be too weak to transfer the tensile stress; the second reason is that the corner points of the irregular-shaped particulates result in stress concentration in the vinyl ester matrix; and the third reason is that the voids in CaSO<sub>4</sub> filler composites (CGV<sub>2</sub> and CGV<sub>3</sub>) are more as comparison to CaCO<sub>3</sub> particulate composites. These three factors are responsible for reducing the tensile strengths of the composites significantly. The tensile strengths are different with both filler materials as their compatibility with the matrix and irregularities in shape are different from each other. The tensile modulus of the CaCO<sub>3</sub> filler is more at 10 wt.% in comparison to CaSO<sub>4</sub> filler. But, at 20 wt.% the tensile

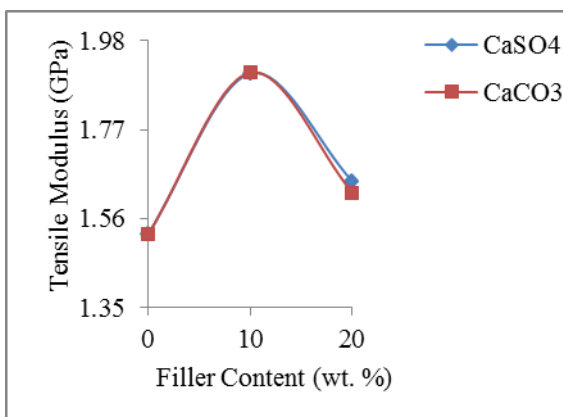
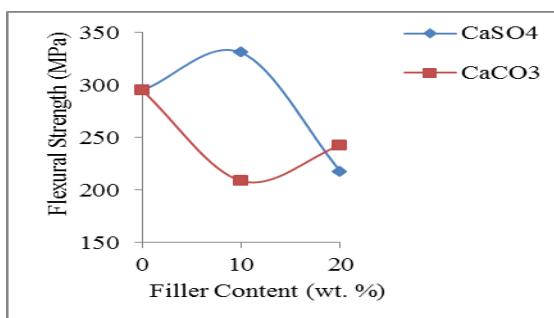


**Fig. 5:** Variation of Tensile Modulus of Composites with Filler Type and Content.

modulus of CaSO<sub>4</sub> is more in comparison to CaCO<sub>3</sub> filler as shown in Figure 5.

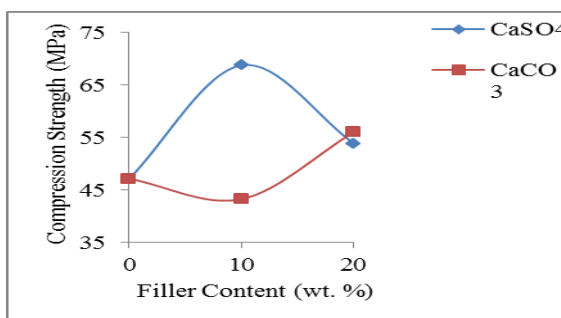
We have seen that tensile strength decreases with increasing the filler content. It happens due to increasing of the brittleness of composite material and increasing of the void fraction. But in case of tensile modulus, tensile strain, i.e., percentage elongation of the composite material is the main cause for increasing the tensile modulus for 10% filler content as compared to 0% and 20% filler content, respectively. The tensile strain of composite material for 10% filler content was less as compared to 0% and 20% filler content.

The flexural test is conducted on the same UTM as per ASTM standard D 2344-84 [25]. Figure 6 shows the comparison of flexural strengths of the composites obtained experimentally from the 3-point bend tests. It is interesting to note that the composite (CGV<sub>2</sub>) with the addition of small amount (10 wt.%) of CaSO<sub>4</sub>, exhibits improved flexural strength compared to the unfilled CSM-E-glass fiber vinyl ester composite. But for this composite sample (CGV<sub>3</sub>) with 20 wt.% of this filler, lower value of the flexural strength is recorded. However, this trend is not found in the composites (CGV<sub>4</sub> and CGV<sub>5</sub>) with CaCO<sub>3</sub> filler, where the flexural strength of the CSM-E-glass fiber vinyl ester system declines at 10 wt.% and then increases at 20 wt.% with filler content but not more than CGV<sub>1</sub> as shown in Figure 6.



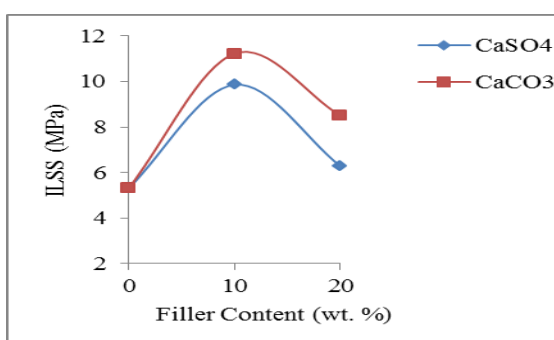
**Fig. 6:** Variation of Flexural Strength of Composites with Filler Type and Content.

The flexural properties are of great importance for any structural element. Composite materials used in structures are prone to fail in bending and, therefore, the development of new composites with improved flexural characteristics is essential. From the results, it may now be suggested that CaCO<sub>3</sub> is a potential candidate to be used as a filler in making high-flexural-strength composites with the increase of the reinforcement of the filler in comparison to CaSO<sub>4</sub> filler. CaSO<sub>4</sub> holds good flexural strength at 10 wt.% filler content, also more than CGV<sub>1</sub> and CGV<sub>4</sub> composites as shown in Figure 6. There may be one reason for this that the void in CGV<sub>2</sub> (5.5996) is less in comparison to CGV<sub>4</sub> (6.4238).



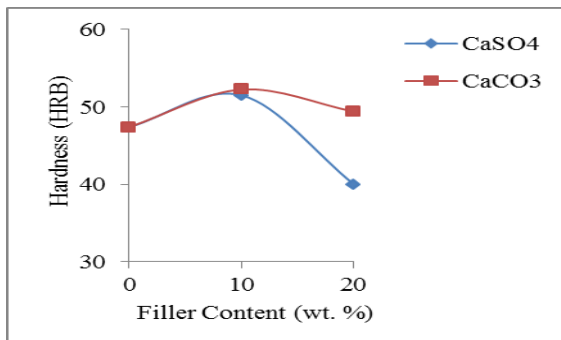
**Fig. 7:** Variation of Compression Strength of Composites with Filler Type and Content.

Figure 7 shows the compressive strengths of the composites obtained experimentally. The pattern for the compressive properties for both the fillers CaSO<sub>4</sub> and CaCO<sub>3</sub> comes almost same as that comes in flexural properties. For composite CGV<sub>2</sub> with the addition of small amount (10 wt.%) of CaSO<sub>4</sub>, exhibits improved compressive strength as compared to the unfilled CSM-E-glass fiber vinyl ester composite but it decreases at 20 wt.% filler content for the same particulate filler. But it does not happen in CaCO<sub>3</sub> filler, for this filler the compressive strength at 10 wt.% decreases firstly and then increases at 20 wt.%, also more than CGV<sub>1</sub> as shown in Figure 7. The compressive strength for CaSO<sub>4</sub> filler holds maximum at 10 wt.% (68.8 MPa).



**Fig. 8:** Variation of ILSS of Composites with Filler Type and Content.

Figure 8 shows the inter-laminar shear strength (ILSS) values of the particulate-filled composites as obtained from experiments. It is seen that there is improvement of ILSS of CSM-E-glass fiber vinyl ester composite with particulate filling irrespective of the filler type. Incorporation of calcium carbonate (CaCO<sub>3</sub>) is seen to have caused the maximum increase in



**Fig. 9:** Variation of Rockwell Hardness of Composites with Filler Type and Content.

the strength compared to the calcium sulfate (CaSO<sub>4</sub>) filler. It can also be noticed that with increase in filler content from 10 to 20 wt.%, there is invariably a drop in the ILSS in both the fillers.

Hardness measurement is done using a Rockwell-hardness tester equipped with a steel

ball indenter (1/16") by applying a load of 100 kgf. Figure 9 shows the hardness of the composites (CGV<sub>1</sub>–CGV<sub>5</sub>) as obtained from the experiments. For composite CGV<sub>1</sub>, the hardness is recorded as 47.4 HRB while for CGV<sub>2</sub> and CGV<sub>3</sub> the values are recorded as 51.5 and 40 HRB respectively. On the other hand, the values for composites CGV<sub>4</sub> and CGV<sub>5</sub> are recorded as 52.25 and 49.4 HRB respectively. From the analysis of the results, we observe that the hardness of the CaCO<sub>3</sub> filler is more in comparison to CaSO<sub>4</sub>. The variations in the properties like tensile strength, tensile modulus, flexural strength, compressive strength, inter-laminar shear strength (ILSS) and hardness are shown in Figures 4–9 respectively.

We have seen from the results of the mechanical properties that there are variations in properties. The reason for these variations is that the mechanical property of composite

material very much depends on the manufacturing technique. Here, composite material is manufactured by hand lay-up technique. In this technique, generally agglomeration and void fraction takes place. Compatibility of filler material with the resin is another reason which affects the mechanical property of the composite material. In the case of ILSS and hardness, void fraction is the main reason for deteriorating the property of composite material at 20% filler content. But in the case of flexural and compressive strength, agglomeration and compatibility of filler material with the resin may be the reason for variation of properties with respect to filler contents.

**Analysis of Experimental Results**

The experimental data for coefficient of friction and specific wear rate (K<sub>s</sub>) for CaCO<sub>3</sub> and CaSO<sub>4</sub> fillers are reported in Table 3 and Table 8, respectively.

**Table 3: Experimental Design for CaCO<sub>3</sub> Using L<sub>27</sub> Array.**

Expt. No.	Velocity (m/s.)	Normal load(N)	Filler content(%)	Sliding distance(m)	COF (μ)	S/N ratio (db)	Wear (mm <sup>3</sup> /Nm)	S/N ratio (db)
1	1.57	20	0	1000	0.67	3.4785	0.0000608	84.322
2	1.57	20	10	3000	0.54	5.3521	0.00000591	104.568
3	1.57	20	20	5000	0.50	6.0206	0.00000382	108.359
4	1.57	40	0	3000	0.69	3.2230	0.0000733	82.698
5	1.57	40	10	5000	0.50	6.0206	0.00000523	105.630
6	1.57	40	20	1000	0.40	7.9588	0.00000186	114.610
7	1.57	60	0	5000	0.72	2.8534	0.0000811	81.820
8	1.57	60	10	1000	0.42	7.5350	0.00000501	106.003
9	1.57	60	20	3000	0.35	9.1186	0.00000108	119.332
10	2.62	20	0	3000	0.62	4.1522	0.0000312	90.117
11	2.62	20	10	5000	0.56	5.0362	0.00000777	102.192
12	2.62	20	20	1000	0.46	6.7448	0.00000592	104.554
13	2.62	40	0	5000	0.65	3.7417	0.0000482	86.339
14	2.62	40	10	1000	0.50	6.0206	0.00000692	103.198
15	2.62	40	20	3000	0.43	7.3306	0.00000451	106.916
16	2.62	60	0	1000	0.47	6.5580	0.0000147	96.654
17	2.62	60	10	3000	0.41	7.7443	0.00000479	106.393
18	2.62	60	20	5000	0.34	9.3704	0.00000345	109.244
19	3.67	20	0	5000	0.59	4.5830	0.0000356	88.971
20	3.67	20	10	1000	0.52	5.6799	0.00000381	108.382
21	3.67	20	20	3000	0.45	6.9357	0.00000282	110.995
22	3.67	40	0	1000	0.50	6.0206	0.0000231	92.728
23	3.67	40	10	3000	0.45	6.9357	0.00000355	108.995
24	3.67	40	20	5000	0.40	7.9588	0.00000271	111.341
25	3.67	60	0	3000	0.52	5.6799	0.0000475	86.466
26	3.67	60	10	5000	0.32	9.8970	0.00000312	110.117
27	3.67	60	20	1000	0.25	12.0412	0.00000241	112.360

The data reported here are the average of two runs. Here, we see that the overall mean for the S/N ratio of the coefficient of friction and specific wear rate is more for CaCO<sub>3</sub> filler in comparison to CaSO<sub>4</sub> which means that the

coefficient of friction and specific wear rate is less in CaCO<sub>3</sub>. The analysis of the experimental data is carried using the software MINITAB 16 specially used for the design of experiment applications.

**Table 4: ANOVA Table for Specific Wear Rate (for CaCO<sub>3</sub>).**

Source	DF	Seq. SS	Adj. SS	Adj. MS	F	P (%)
A	2	42.41	42.41	21.21	2.79	1.381
B	2	38.00	38.00	19.00	2.50	1.237
C	2	2674.98	2674.98	1337.49	176.10	87.111
D	2	20.33	20.33	10.16	1.34	0.662
A*B	4	37.20	37.20	9.30	1.22	1.211
A*C	4	190.94	190.94	47.73	6.29	6.218
B*C	4	21.33	21.33	5.33	0.70	0.695
Residual Error	6	45.57	45.57	7.59		1.484
Total	26	3070.76				100.00

**Table 5: Response Table for Specific Wear Rate (for CaCO<sub>3</sub>)**

Level	A	B	C	D
1	100.82	100.27	87.79	102.53
2	100.62	101.38	106.16	101.83
3	103.37	103.15	110.86	100.45
Delta	2.75	2.88	23.07	2.09
Rank	3	2	1	4

of friction and specific wear rate of the composite specimens CGV<sub>1</sub>, CGV<sub>4</sub> and CGV<sub>5</sub>. The analysis of the results gives the combination factors resulting in minimum coefficient of friction and specific wear rate of the composites. Analysis of these results leads to the conclusion that factors combination A<sub>3</sub>, B<sub>3</sub>, C<sub>3</sub> and D<sub>1</sub> gives minimum coefficient of friction as shown in Figure 10. Similarly, the combination factors A<sub>3</sub>, B<sub>3</sub>, C<sub>3</sub> and D<sub>1</sub> give minimum specific wear rate as shown in Figure 11.

Figures 10 and 11 for CaCO<sub>3</sub> show graphically the effect of four control factors on coefficient

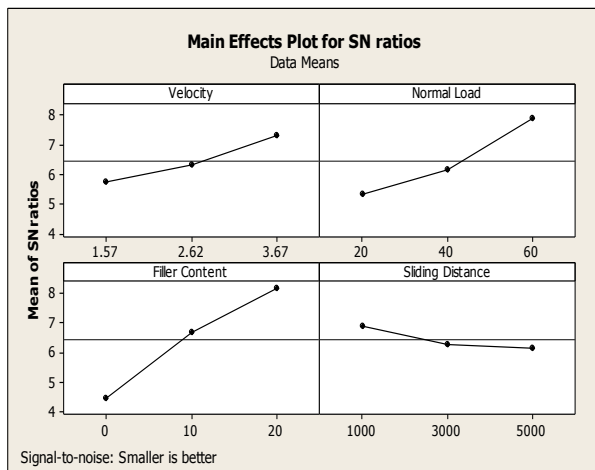


**Fig. 10: Effect of Control Factor on Coefficient of Friction (for CaCO<sub>3</sub>).**

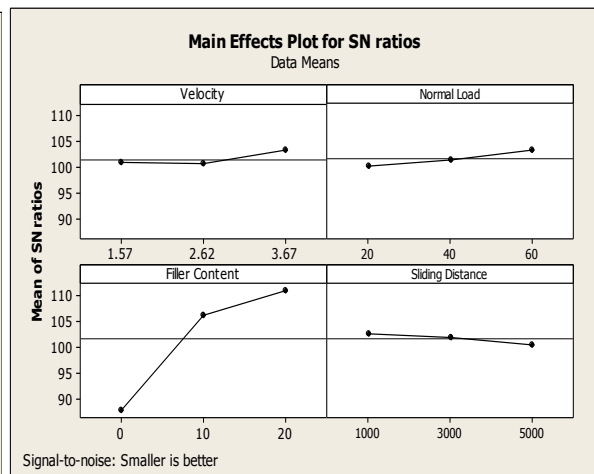


**Fig. 11: Effect of Control Factor on Specific Wear Rate (for CaCO<sub>3</sub>).**

On the other hand, for CaSO<sub>4</sub> Figures 12 and 13 show graphically the effect of four control factors on coefficient of friction and specific wear rate of the composite specimens CGV<sub>1</sub>, CGV<sub>2</sub> and CGV<sub>3</sub>. Analysis of these results leads to the conclusion that factors

combination A<sub>3</sub>, B<sub>3</sub>, C<sub>2</sub> and D<sub>1</sub> gives minimum coefficient of friction as shown in Figure 12. Similarly, the combination of factors A<sub>3</sub>, B<sub>3</sub>, C<sub>2</sub> and D<sub>1</sub> gives minimum specific wear rate as shown in Figure 13.

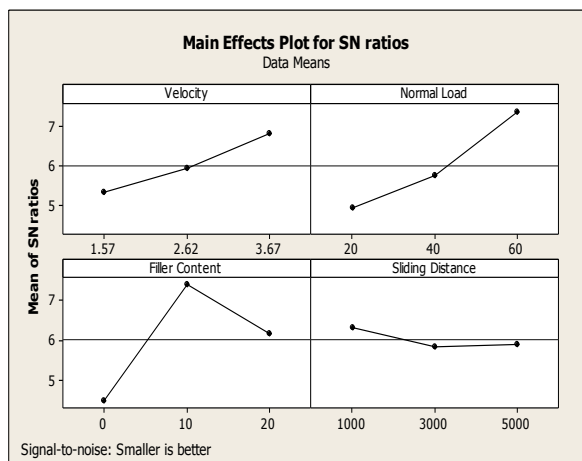


Fig. 12: Effects of Control Factor for Coefficient of Friction (for CaSO<sub>4</sub>).

In order to understand the impact of various control factors like velocity (A), normal load (B), filler content (C) and sliding distance (D) and interaction on the response of experimental data it is desirable to develop the analysis of variance (ANOVA) to find the significant factors as well as interactions. ANOVA allows analyzing the influence of each variable on the total variance of the results. For CaCO<sub>3</sub>, Table 4 shows the results of ANOVA for the specific wear rate and Table 6 shows the results of ANOVA for coefficient of friction and for CaSO<sub>4</sub>, Table 9 shows the results of ANOVA for the specific

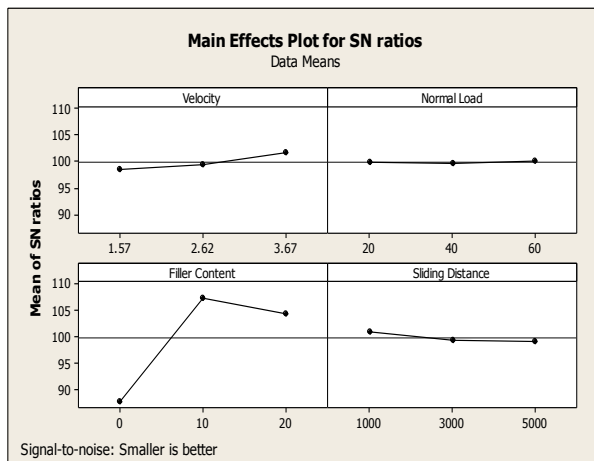


Fig. 13: Effect of Control Factor on Specific Wear Rate (for CaSO<sub>4</sub>).

wear rate and Table 11 shows the results of ANOVA for coefficient of friction.

For filler CaCO<sub>3</sub>, from the analysis of ANOVA and response Table 5 of the S/N ratio of specific wear rate, it is observed that the control factor filler content (C) has major impact on the specific wear rate followed by normal load (B), velocity (A) and sliding distance (D). It means that with increasing the filler content, velocity and normal load the specific wear rate decreases, i.e., increase the wear resistance as observed from Figures 11 and 16.

Table 6: ANOVA Table for Coefficient of Friction (for CaCO<sub>3</sub>).

Source	DF	Seq. SS	Adj. SS	Adj. MS	F	P (%)
A	2	11.438	11.438	5.7189	15.08	9.457
B	2	30.212	30.212	15.1059	39.83	24.979
C	2	62.021	62.021	31.0105	81.76	51.277
D	2	2.775	2.775	1.3876	3.66	2.294
A*B	4	3.606	3.606	0.9016	2.38	2.981
A*C	4	2.609	2.609	0.6522	1.72	2.157
B*C	4	6.015	6.015	1.5037	3.96	4.973
Residual error	6	2.276	2.276	0.3793		1.882
Total	26	120.952				100.00

**Table 7: Response Table for Coefficient of Friction (for CaCO<sub>3</sub>).**

Level	A	B	C	D
1	5.729	5.331	4.477	6.893
2	6.300	6.135	6.691	6.275
3	7.304	7.866	8.164	6.165
Delta	1.575	2.535	3.688	0.728
Rank	3	2	1	4

In the same way, from the ANOVA Table 6 with the analysis of ANOVA and response Table 7 of the S/N ratio of coefficient of friction, it is observed that the filler content (C) has major influence followed by normal load (B), velocity (A) and sliding distance (D) as for the specific wear rate.

For filler CaSO<sub>4</sub>, from the analysis of ANOVA and response Table 10 of the S/N ratio for specific wear rate, it is observed that the control factor filler content (C) has major impact on specific wear rate which is followed by the velocity (A), sliding distance (D) and the normal load (B). It means that for filler CaSO<sub>4</sub>, with the increases of the filler content, velocity and sliding distance, the specific wear rate decreases, i.e., the wear resistance is good as observed from Figures 13 and 17.

But from the figures, we also observe that for CaSO<sub>4</sub>, the filler content plays adverse effect when filler content is increased from 10 to 20 wt.%. At 10 wt.% for CaSO<sub>4</sub>, the specific wear rate is decreased and for 20 wt.%, it further decreases.

The coefficient of friction and specific wear rate behavior of CaCO<sub>3</sub> filler composites is shown in Figures 14 and 15 respectively. From these figures, we analyze that both coefficient of friction and specific wear rate decrease with the filler content.

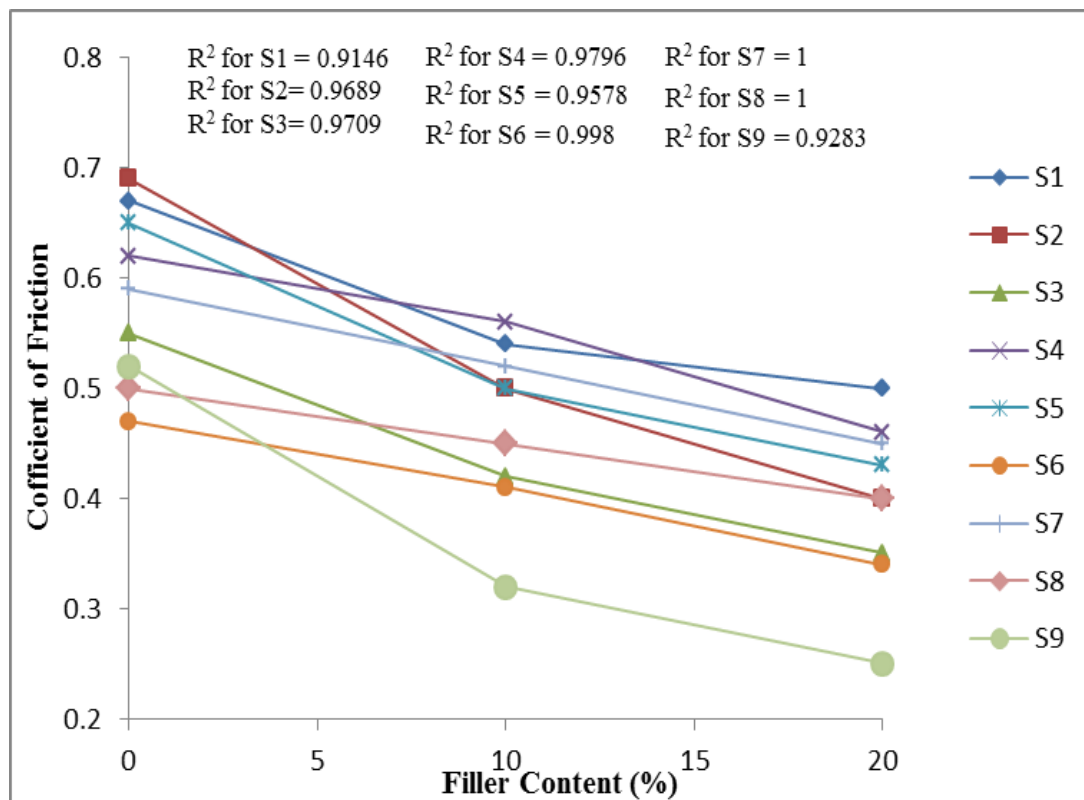


**Fig. 14: Variation of Coefficient of Friction with Filler Content (for CaCO<sub>3</sub>).**

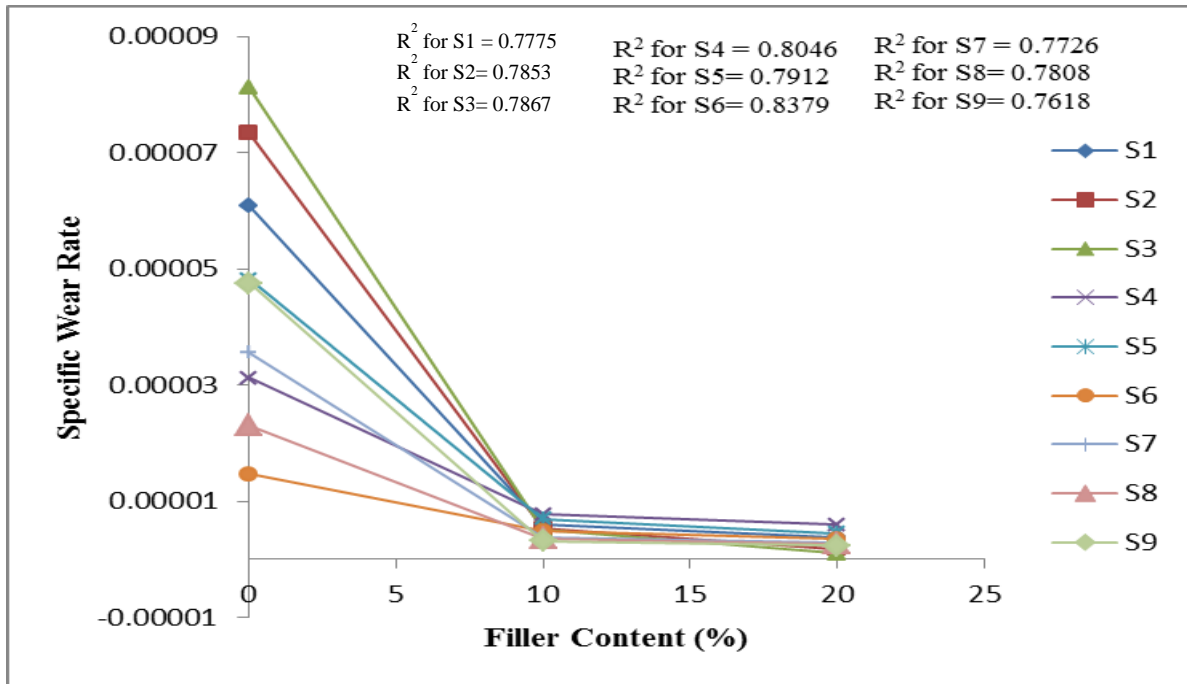


Fig. 15: Variation of Specific Wear Rate with Filler Content (for CaCO<sub>3</sub>).

Table 8: Experimental Design for CaSO<sub>4</sub> Using L<sub>27</sub> Array.

Expt. No.	Velocity (m/s)	Normal load (N)	Filler content (%)	Sliding distance (m)	COF (μ)	S/N ratio (db)	Wear (mm <sup>3</sup> /Nm)	S/N ratio (db)
1	1.57	20	0	1000	0.67	3.4785	0.0000608	84.322
2	1.57	20	10	3000	0.53	5.5145	0.0000455	106.840
3	1.57	20	20	5000	0.60	4.4370	0.0000482	106.339
4	1.57	40	0	3000	0.69	3.2230	0.0000733	82.698
5	1.57	40	10	5000	0.43	7.3306	0.0000423	107.473
6	1.57	40	20	1000	0.54	5.3521	0.0000548	105.224
7	1.57	60	0	5000	0.72	2.8534	0.0000811	81.820
8	1.57	60	10	1000	0.38	8.4043	0.0000381	108.382
9	1.57	60	20	3000	0.43	7.3306	0.0000592	104.554
10	2.62	20	0	3000	0.62	4.1522	0.0000312	90.117
11	2.62	20	10	5000	0.50	6.0206	0.0000686	103.274
12	2.62	20	20	1000	0.58	4.7314	0.0000712	102.950
13	2.62	40	0	5000	0.65	3.7417	0.0000482	86.339
14	2.62	40	10	1000	0.46	6.7448	0.0000602	104.408
15	2.62	40	20	3000	0.52	5.6799	0.0000785	102.103
16	2.62	60	0	1000	0.47	6.5580	0.0000147	96.654
17	2.62	60	10	3000	0.38	8.4043	0.0000468	106.595
18	2.62	60	20	5000	0.43	7.3306	0.0000815	101.777
19	3.67	20	0	5000	0.59	4.5830	0.0000356	88.971
20	3.67	20	10	1000	0.48	6.3752	0.0000352	109.069
21	3.67	20	20	3000	0.55	5.1927	0.0000048	106.375
22	3.67	40	0	1000	0.50	6.0206	0.0000231	92.728
23	3.67	40	10	3000	0.43	7.3306	0.0000322	109.843
24	3.67	40	20	5000	0.48	6.3752	0.0000525	105.597
25	3.67	60	0	3000	0.52	5.6799	0.0000475	86.466
26	3.67	60	10	5000	0.30	10.4576	0.0000305	110.314
27	3.67	60	20	1000	0.35	9.1186	0.0000055	105.193

**Table 9: ANOVA Table for Specific Wear Rate (for CaSO<sub>4</sub>).**

Source	DF	Seq. SS	Adj. SS	Adj. MS	F	P (%)
A	2	43.73	43.73	21.86	4.83	1.932
B	2	1.63	1.63	0.82	0.18	0.072
C	2	2006.85	2006.85	1003.43	221.81	88.647
D	2	17.83	17.83	8.92	1.97	0.788
A*B	4	32.44	32.44	8.11	1.79	1.433
A*C	4	124.95	124.95	31.24	6.91	5.519
B*C	4	9.28	9.28	2.32	0.51	0.409
Residual error	6	27.14	27.14	4.52		1.199
Total	26	2263.86				100.00

**Table 10: Response Table for Specific Wear Rate (for CaSO<sub>4</sub>).**

Level	A	B	C	D
1	98.63	99.81	87.79	100.99
2	99.36	99.60	107.36	99.51
3	101.62	100.19	104.46	99.10
Delta	2.99	0.59	19.56	1.89
Rank	2	4	1	3

In the same way, from ANOVA Table 11, the analysis of the ANOVA and the response

Table 12 for coefficient of friction, it is observed that the filler content (C) has major influence followed by the normal load (B), velocity (A) and the sliding distance (D). From Figure 12 for CaSO<sub>4</sub>, it is observed that the coefficient of friction also increases with the increase of the filler content. It means that in 10 wt.% the coefficient of friction is less in comparison to 20 wt.%, i.e., the reinforcement of the CaSO<sub>4</sub> filler at 10 wt.% is more wear resistant.

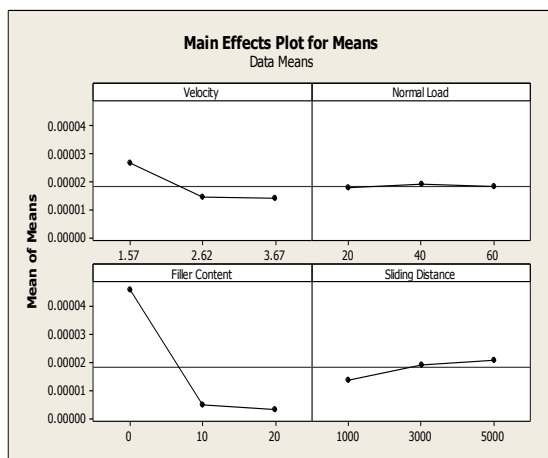


**Fig. 16: Effect of Mean Factor on Specific Wear Rate (for CaCO<sub>3</sub>).**

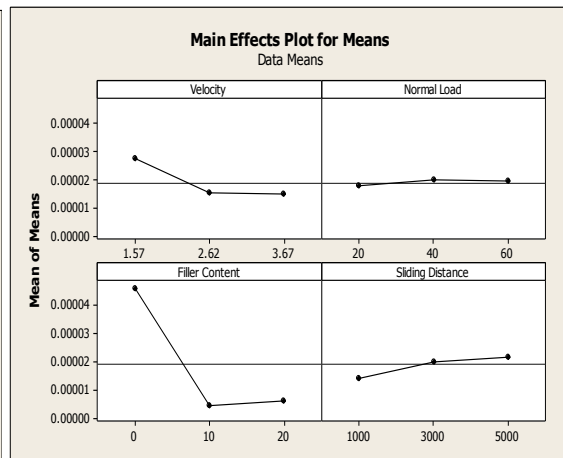


**Fig. 17: Effect of Mean Factor on Specific Wear Rate (for CaSO<sub>4</sub>).**

**Table 11: ANOVA Table for Coefficient of Friction (for CaSO<sub>4</sub>).**

Source	DF	Seq. SS	Adj. SS	Adj. MS	F	P (%)
A	2	9.794	9.794	4.8972	8.66	10.950
B	2	26.960	26.960	13.4799	23.85	30.143
C	2	38.735	38.735	19.3675	34.27	43.309
D	2	1.186	1.186	0.5930	1.05	1.326
A*B	4	1.921	1.921	0.4801	0.85	2.148
A*C	4	2.633	2.633	0.6583	1.16	2.944
B*C	4	4.819	4.819	1.2048	2.13	5.388
Residual Error	6	3.391	3.391	0.5652		3.791
Total	26	89.439				100.00

**Table 12:** Response Table for Coefficient of Friction (for CaSO<sub>4</sub>).

Level	A	B	C	D
1	5.325	4.943	4.477	6.309
2	5.929	5.755	7.398	5.834
3	6.793	7.349	6.172	5.903
Delta	1.468	2.406	2.921	0.475
Rank	3	2	1	4

The coefficient of friction and specific wear rate behavior of CaSO<sub>4</sub> filler composites are shown in Figures 18 and 19 respectively. From these figures, we analyze that both the coefficient of friction and specific wear rate decrease with the filler content up to 10 wt.% filler content but as we further increase the filler content, then it increases.

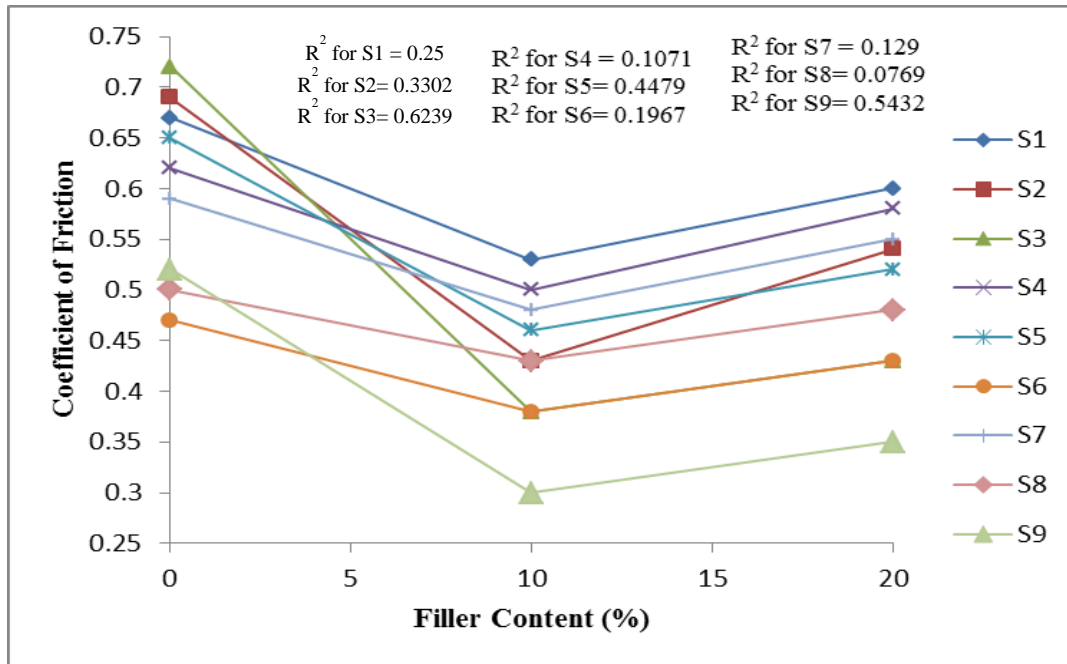


**Fig. 18:** Variation of Coefficient of Friction with Filler Content (for CaSO<sub>4</sub>).

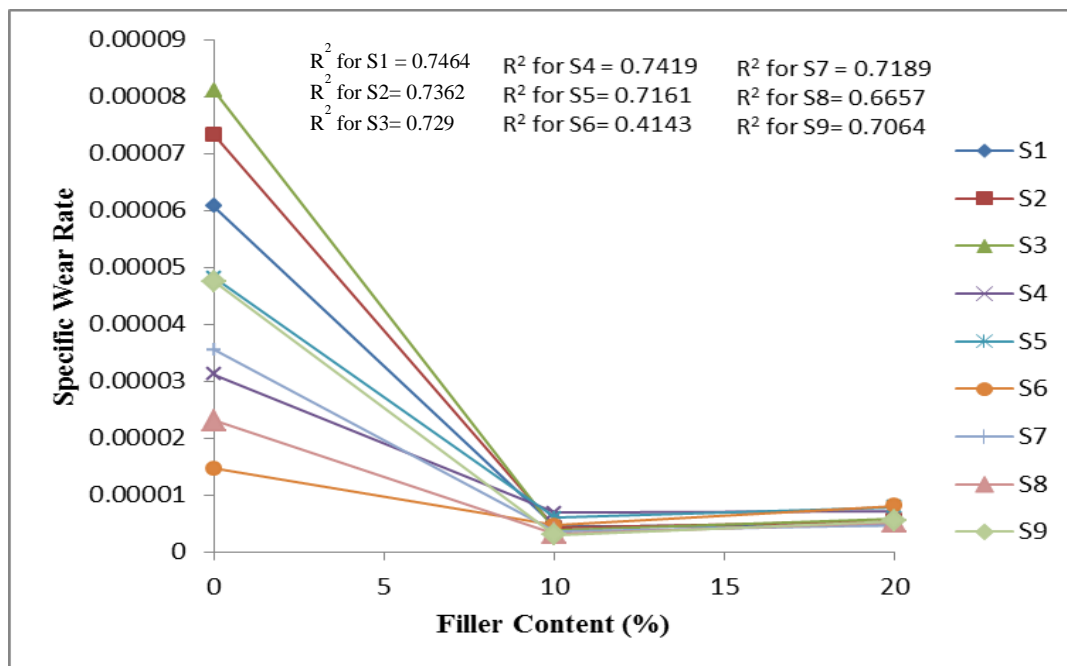


**Fig. 19:** Variation of Specific Wear Rate with Filler Content (for CaSO<sub>4</sub>).

### Surface Morphology

Figure 20(a-c) are the SEM pictures of composites for maximum, minimum and nominal wear test conditions for  $\text{CaCO}_3$  filled vinyl ester composites with CSM-E-glass fiber. It has been found from the experimental analysis that the maximum wear occurs at

1.57 m/s, 60 N, 0 wt.%, 5000 m test parameter conditions, the minimum wear occurs at 1.57 m/s, 60 N, 20 wt.%, 3000 m test parameter conditions and the nominal wear occurs at 2.62 m/s, 40 N, 10 wt.%, 1000 m test parameter conditions as shown in the Figure 20(a-c).

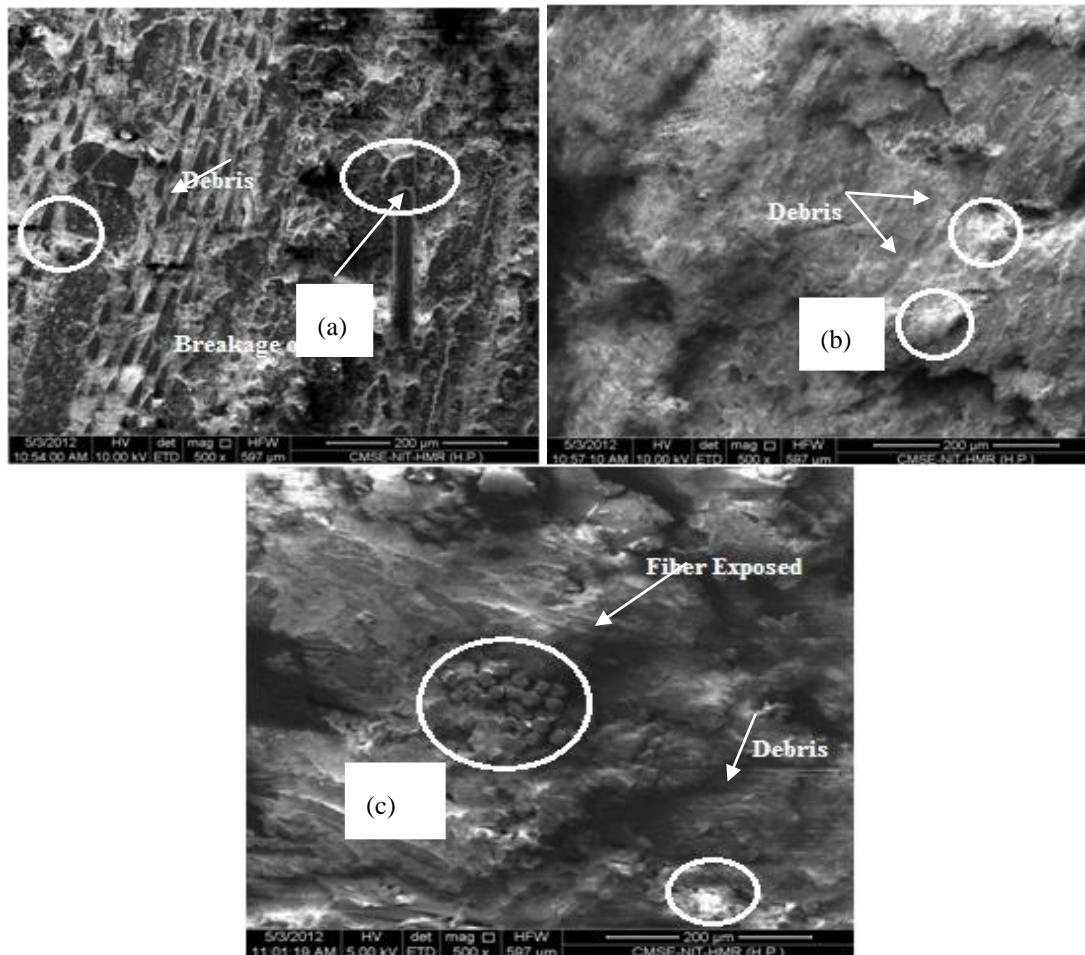


**Fig. 20:** SEM Pictures of Composites at: (a) 1.57 m/s, 60 N, 0 wt.%, 5000 m, (b) 1.57 m/s, 60 N, 20 wt.%, 3000 M, (c) 2.62 m/s, 40 N, 10 wt.%, 1000 m (for  $\text{CaCO}_3$  Filled Vinyl Ester Composites with CSM-E-Glass Fiber).

The micrograph in Figure 20 a and c of composites shows small patches of debris. It is seen that worn surfaces have more fibers exposed and more of debris in the form layers is accumulated which resulted in breakage of fibers and hence increased wear rate. But, on the other hand Figure 20b shows less exposure of CSM-E-glass fiber, covered with debris and hence shows less wear.

Similarly, Figure 21(a-c) are the SEM pictures of composites for maximum, minimum and nominal wear test conditions for  $\text{CaSO}_4$  filled vinyl ester composites with CSM-E-glass fiber. It has been found from the experimental analysis that the maximum wear occurs at 1.57 m/s, 60 N, 0 wt.%, 5000 m test parameter conditions, the minimum wear occurs at 3.67 m/s, 60 N, 10 wt.%, 5000 m test parameter conditions and the nominal wear occurs at 2.62 m/s, 60 N, 0 wt.%, 1000 m test parameter conditions as shown in Figure 21(a-c).

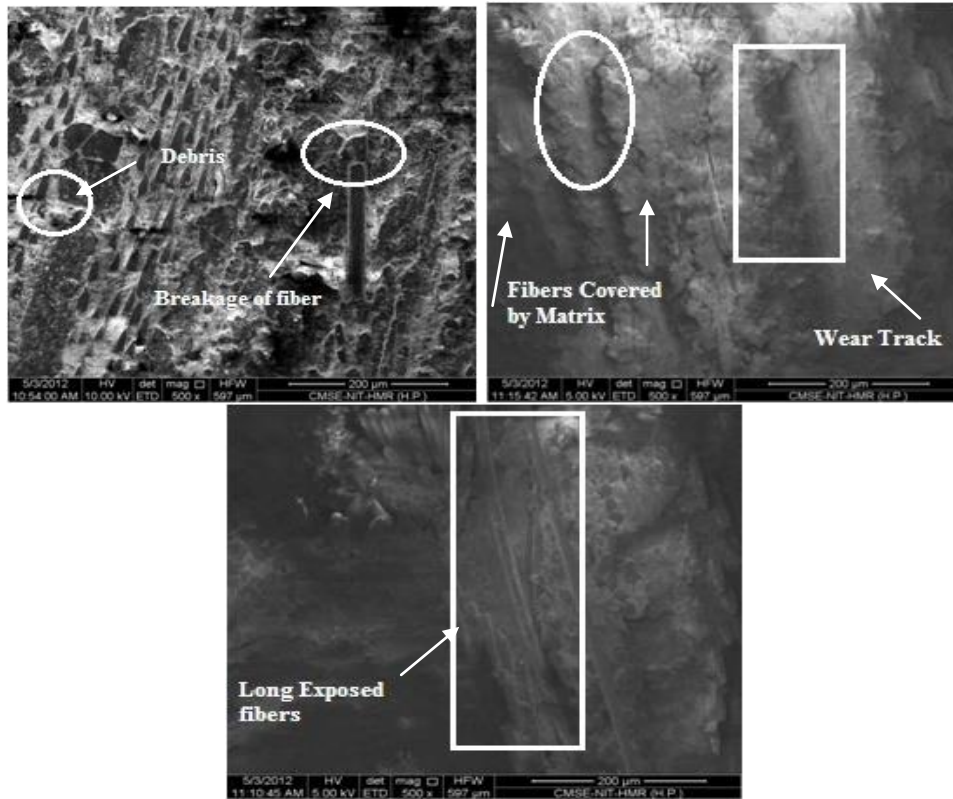


**Fig. 21:** SEM Pictures of Composites at: (a) 1.57 m/s, 60 N, 0 wt.%, 5000 m, (b) 3.67 m/s, 60 N, 10 wt.%, 5000 m, (c) 2.62 m/s, 60 N, 0 wt.%, 1000 m (for  $\text{CaSO}_4$  Filled Vinyl Ester Composites with CSM-E-Glass Fiber).

Figure 21a and c show maximum fiber breakage and exposures, which resulted in the higher wear rate. Figure 17b shows lesser amount of fiber breakage, more masking of fibers and distribution of matrix uniformly, which resulted in the lesser wear rate. The fibers are covered by the matrix and those exposed having patches of debris stuck to them and show lesser wear as shown in Figure 21b.

**Confirmation Experiments**

The confirmation experiment is the final step in the design of experiments process. It predicts and verifies the improvements in the

$$\begin{aligned} \bar{\eta}_{\text{CaCO}_3} = & \bar{T} + (\bar{A}_2 - \bar{T}) + (\bar{B}_1 - \bar{T}) + (\bar{C}_3 - \bar{T}) + (\bar{D}_2 - \bar{T}) + [(\bar{A}_2\bar{B}_1 - \bar{T}) - (\bar{A}_2 - \bar{T}) - \\ & (\bar{B}_1 - \bar{T})] + [(\bar{B}_1\bar{C}_3 - \bar{T}) - (\bar{B}_1 - \bar{T}) - (\bar{C}_3 - \bar{T})] \end{aligned} \tag{4}$$

where,  $\bar{\eta}_{\text{CaCO}_3}$  is the predicted average of  $\text{CaCO}_3$  for coefficient of friction,  $\bar{T}$  is the overall experimental average,  $\bar{A}_2\bar{B}_1$ ,  $\bar{B}_1\bar{C}_3$  and  $\bar{D}_2$  is the mean response for factors and

observed values through the use of optimal combination level of control factors. For filler  $\text{CaCO}_3$ , the confirmation experiment was performed by taking an arbitrary set of factor combination  $A_2 B_1 C_3 D_2$  to predict the coefficient of friction and for specific wear rate factor setting is  $A_1 B_2 C_3 D_2$ . For filler  $\text{CaSO}_4$ , we are taking the same arbitrary set of factor combination for the coefficient of friction and specific wear rate respectively. Now, the estimated S/N ratio for coefficient of friction can be calculated with the help of the following predictive equation:

interactions at designed levels. By combining all the terms Eq. (4) reduces to:

$$\bar{\eta}_{\text{CaCO}_3} = \bar{A}_2\bar{B}_1 + \bar{B}_1\bar{C}_3 + \bar{D}_2 - \bar{B}_1 - \bar{T} \tag{5}$$

A new combination of factor levels  $A_2 B_1 C_3 D_2$  is used to predict the S/N ratio of coefficient of friction through predictive

equation and is found to be  $\bar{\eta}_{CaCO_3} = 6.3772$  db. Similarly, a predictive equation is

$$\bar{\eta}_{CaCO_3} = \bar{T} + (\bar{A}_1 - \bar{T}) + (\bar{B}_2 - \bar{T}) + (\bar{C}_3 - \bar{T}) + (\bar{D}_2 - \bar{T}) + [(\bar{A}_1\bar{B}_2 - \bar{T}) - (\bar{A}_1 - \bar{T}) - (\bar{B}_2 - \bar{T})] + [(\bar{B}_2\bar{C}_3 - \bar{T}) - (\bar{B}_2 - \bar{T}) - (\bar{C}_3 - \bar{T})] \quad (6)$$

where,  $\bar{\eta}_{CaCO_3}$  is the predictive average of CaCO<sub>3</sub> for specific wear rate,  $\bar{T}$  is the overall experimental average,  $\bar{A}_1\bar{B}_2$ ,  $\bar{B}_2\bar{C}_3$  and  $\bar{D}_2$  is the mean response for factors and interactions at designed levels. By combining all the terms Eq. (6) reduces to:

$$\bar{\eta}_{CaCO_3} = \bar{A}_1\bar{B}_2 + \bar{B}_2\bar{C}_3 + \bar{D}_2 - \bar{B}_2 - \bar{T} \quad (7)$$

A new combination of factor levels A<sub>1</sub> B<sub>2</sub> C<sub>3</sub> D<sub>2</sub> is used to predict the S/N ratio of specific wear rate through predictive Eq. (7) and is found to be  $\bar{\eta}_{CaCO_3} = 110.7783$  db. The resulting equations seem to be capable of

$$\bar{\eta}_{CaSO_4} = \bar{T} + (\bar{A}_2 - \bar{T}) + (\bar{B}_1 - \bar{T}) + (\bar{C}_3 - \bar{T}) + (\bar{D}_2 - \bar{T}) + [(\bar{A}_2\bar{B}_1 - \bar{T}) - (\bar{A}_2 - \bar{T}) - (\bar{B}_1 - \bar{T})] + [(\bar{A}_2\bar{C}_3 - \bar{T}) - (\bar{A}_2 - \bar{T}) - (\bar{C}_3 - \bar{T})] \quad (8)$$

where,  $\bar{\eta}_{CaSO_4}$  is the predicted average of CaSO<sub>4</sub> for coefficient of friction,  $\bar{T}$  is the overall experimental average  $\bar{A}_2\bar{B}_1$ ,  $\bar{A}_2\bar{C}_3$  and  $\bar{D}_2$  is the mean response for factors and interactions at designed levels. By combining all the terms, Eq. (8) reduces to:

$$\bar{\eta}_{CaSO_4} = \bar{A}_2\bar{B}_1 + \bar{A}_2\bar{C}_3 + \bar{D}_2 - \bar{A}_2 - \bar{T} \quad (9)$$

$$\bar{\eta}_{CaSO_4} = \bar{T} + (\bar{A}_1 - \bar{T}) + (\bar{B}_2 - \bar{T}) + (\bar{C}_3 - \bar{T}) + (\bar{D}_2 - \bar{T}) + [(\bar{A}_1\bar{B}_2 - \bar{T}) - (\bar{A}_1 - \bar{T}) - (\bar{B}_2 - \bar{T})] + [(\bar{A}_1\bar{C}_3 - \bar{T}) - (\bar{A}_1 - \bar{T}) - (\bar{C}_3 - \bar{T})] \quad (10)$$

where,  $\bar{\eta}_{CaSO_4}$  is the predictive average of CaSO<sub>4</sub> for specific wear rate,  $\bar{T}$  is the overall experimental average  $\bar{A}_1\bar{B}_2$ ,  $\bar{A}_1\bar{C}_3$  and  $\bar{D}_2$  is the mean response for factors and interactions at designed levels. By combining all the terms, Eq. (10) reduces to:

$$\bar{\eta}_{CaSO_4} = \bar{A}_1\bar{B}_2 + \bar{A}_1\bar{C}_3 + \bar{D}_2 - \bar{A}_1 - \bar{T} \quad (11)$$

developed for estimating S/N ratio of specific wear rate as shown in Eq. (6).

predicting the coefficient of friction and specific wear rate. An error of 4.11% for the S/N ratio of the coefficient of friction and 3.05% for the S/N ratio of the specific wear rate is observed.

For filler CaSO<sub>4</sub>, the confirmation experiment was performed by taking an arbitrary set of factor combination A<sub>2</sub> B<sub>1</sub> C<sub>3</sub> D<sub>2</sub> as was taken for the CaCO<sub>3</sub> filler to predict the coefficient of friction and for specific wear rate factor setting is A<sub>1</sub> B<sub>2</sub> C<sub>3</sub> D<sub>2</sub>. Now, the estimated S/N ratio for coefficient of friction can be calculated with the help of the following predictive equation:

A new combination of factor levels A<sub>2</sub> B<sub>1</sub> C<sub>3</sub> D<sub>2</sub> is used to predict the S/N ratio of coefficient of friction through predictive equation and is found to be  $\bar{\eta}_{CaSO_4} = 4.7714$  db. Similarly, a predictive equation is developed for estimating S/N ratio of specific wear rate as shown in Eq. (10).

A new combination of factor levels A<sub>1</sub> B<sub>2</sub> C<sub>3</sub> D<sub>2</sub> is used to predict the S/N ratio of specific wear rate through predictive Eq. (11) and is found to be  $\bar{\eta}_{CaSO_4} = 104.8519$  db. The resulting equations seem to be capable of predicting the coefficient of friction and specific wear rate. An error of 5.79% for the S/N ratio of the coefficient of friction and 4.89% for the S/N ratio of the specific wear rate is observed.

## CONCLUSIONS

An experimental study has been carried out for friction and dry sliding wear of vinyl ester matrix reinforced with CSM-E-glass fiber with fillers  $\text{CaCO}_3$  and  $\text{CaSO}_4$  sliding against smooth stainless steel counterface using Taguchi experimental design. Taguchi's design of experiment method can be used to analyze the coefficient of friction and the dry sliding wear of polymer matrix composites as presented in this research paper. The following conclusions can be drawn from the present study:

1. Fabrication of the hybrid composites consisting of CSM-E-glass fiber in vinyl ester matrix-filled particulate filler  $\text{CaCO}_3$  and  $\text{CaSO}_4$  is possible.
2. It is seen that in all the samples for both the fillers  $\text{CaCO}_3$  and  $\text{CaSO}_4$  irrespective of the filler material, the tensile strength of the composite decreases with the increase of the filler content.
3. For filler  $\text{CaCO}_3$  the properties such as flexural and compression strength are higher in 20 wt.% filler content whereas the properties such as tensile strength, ILSS and Rockwell hardness (HRB) of the composite are more at 10 wt.% of the composite in the  $\text{CaCO}_3$  filler content.
4. For filler  $\text{CaSO}_4$  the properties, i.e., tensile strength, flexural strength, compressive strength, inter-laminar shear strength and hardness are higher in 10 wt.% of the composite in comparison to the 20 wt.% of filler content.
5. The coefficient of friction decreases with the addition of 10 – 20 wt.% of  $\text{CaCO}_3$  and the wear resistance increases with the addition of 10–20 wt% of  $\text{CaCO}_3$  filler. Filler content (C) is the main factor that has the highest physical and statistical significance in influencing the coefficient of friction and specific wear rate followed by the normal load (B), velocity (A) and sliding distance (D).
6. For filler  $\text{CaSO}_4$ , the coefficient of friction decreases at 10 wt.% and then increases at 20 wt.% filler content. It means that the filler  $\text{CaSO}_4$  is more wear resistant at 10 wt.%. Filler content (C) is again the main factor that has the highest physical and statistical significance influencing the coefficient of friction followed by normal load (B), velocity (C) and the sliding

distance (D). For specific wear rate, filler content is also the main factor that has the highest significance followed by velocity (A), sliding distance (B) and the normal load (D).

7. The predictive equations based on Taguchi approach are successfully used for the prediction of effect of various factors and predicted results are consistent with experimental observations.

## ACKNOWLEDGMENTS

This work is based upon the experimental work and is carried out in the National Institute of Technology, Hamirpur. Firstly, the authors would like to thank Lord Shiva. They would also like to thank NIT, Hamirpur, for their able support. The authors would also like to thank Vivek Ramdas Desale, Akant Kumar Singh and Deepak Jain (Asst. Prof. Lovely Professional University) for their valuable support in between the work.

## REFERENCES

1. Kishore P. Sampathkumaran, S. Seetharamu, A. Murali, et al. On the SEM features of glass-epoxy composite system subjected to dry sliding wear. *Wear* 2001;247:208–213p.
2. S. K. Biswas, K. Vijayan. Friction and wear of PTFE-A review. *Wear* 1992;158:193p.
3. J. Bijwe, J. Indumathi, J. J. Rajesh, et al. Friction and wear behavior of polyetherimide composites in various wear modes. *Int. J. Wear* 2001;249:715–726p.
4. N. S. M. EI-Tayeb, B.F Yousif, T.C Yap. Tribological studies of polyester reinforced with CSM 450-R-glass fiber sliding against smooth stainless steel counterface. *Wear* 2006;261:443–452p.
5. N. S. M. EI-Tayeb, Mostafa. The effect of laminate orientations on friction and wear mechanisms of glass reinforced polyester composite. *Int. J. Wear* 1996;195:186–191p.
6. N. S. M. EI-Tayeb, R. M. Gadelrab. Friction and wear properties of E-glass fiber reinforced epoxy composites under different sliding contact conditions. *Int. J. Wear* 1996;192:112–117p.
7. H. Pihtili, N. Tosun. Investigation of the wear behavior of a glass-fiber-reinforced

- composite and plain polyester resin. *Int. J. Compos. Sci. Technol.* 2002;62: 367–370p.
8. S. Bahadur, Y. Zheng. Mechanical and tribological behavior of polyester reinforced with short glass fiber. *Int. J. Wear* 1990;137:251–266p.
  9. T. Tsukizoc, N. Ohmae. Friction and wear of advanced composite materials. *Int. J. Fiber Sci. Technol.* 1983; 18: 265–286p.
  10. S. Bahadur, V. K Polineni. Tribological studies of glass fabric-reinforced polyamide composite filled with CuO and PTFE. *Int. J. Wear* 1996; 200: 95–104p.
  11. H. Pihtili, N. Tosun. Effect of load and speed on the wear behavior of woven glass fabrics and aramid fiber-reinforced composites. *Int. J. Wear* 2002; 252: 979–984p.
  12. S. R. Chauhan, A. Kumar, I. Singh. Sliding friction and wear behavior of vinyl ester and its composites under dry and water lubricated sliding conditions. *Materials and Design* 2010; 31: 2745–2751p.
  13. K. Friedrich, Z. Lu, A. M. Hager. Recent advances in polymer composites tribology. *Wear* 1995;190:139–44p.
  14. N. H. Sung, N. P. Suh. Effect of fiber orientation on friction and wear of fiber reinforced polymeric composites. *Wear* 1979;53:129–141p.
  15. S. R. Chauhan, A. Kumar, I. Singh, et al. Effect of fly ash content on friction and dry sliding wear behavior of glass fiber reinforced polymer composites – A Taguchi approach. *Journal of Minerals & Materials Characterization & Engineering* 2010;9:365–387p.
  16. N. S. M. El-Tayeb, B. F. Yousif, T. C. Yap. An investigation on worn surfaces of chopped glass fiber reinforced polyester through SEM observations. *Tribol Int.* 2008;41:331–340p.
  17. Leonard Hollaway. *Handbook of Polymer Composites for Engineers*. New Delhi: Jaico Publishing House; 1995.
  18. P. J. Ross. *Taguchi Techniques for Quality Engineering*. New York: Mc Graw Hill; 1995.
  19. S. H. Park. *Robust Design & Analysis for Quality Engineering*. London: Chapman & Hall; 1996.
  20. M. S. Phadke. *Quality Engineering Using Robust Design*. New Jersey: Prentice Hall Englewood & Cliffs; 1989.
  21. G. Taguchi. *Introduction to Quality Engineering*. Tokyo: Asian Productivity Organization; 1990.
  22. K. R. Roy. *A Primer on Taguchi Method*. New York: Van Nostrand Reinhold; 1990.
  23. B. D. Agarwal, L. J. Broutman. *Analysis and Performance of Fiber Composites*, 2nd edn. John Wiley and Sons, Inc.; 1990.
  24. Tensile properties of fiber-resin composites ASTM D 3039–76. *American National Standard*. 1976.
  25. American society for testing and materials (ASTM). In: Standard test method for apartment interlaminar shear strength of parallel fiber composites by short beam method, ASTM D 2344-84. West Conshohocken (PA): *Annual Book of ASTM Standards*. ASTM. 1984. 15–17p.